Effect of Crevice Corrosion Inhibitors on the Passivity of Alloy 22

Mauricio Rincón Ortíz, Martín A. Rodríguez and Ricardo M. Carranza

J. Electrochem. Soc. 2012, Volume 159, Issue 11, Pages C469-C475.
doi: 10.1149/2.040211jes

Journal of The Electrochemical Society, **159** (11) C469-C475 (2012)
0013-4651/2012/159(11)/C469/7/$28.00 © The Electrochemical Society

Effect of Crevice Corrosion Inhibitors on the Passivity of Alloy 22

Mauricio Rincón Ortíz,[a] Martín A. Rodríguez,[b,c,z] and Ricardo M. Carranza[b]

[a]*Department of Chemical and Biomolecular Engineering, University of Akron, Akron, Ohio 44325, USA*
[b]*Gerencia Materiales, Comisión Nacional de Energía Atómica, Instituto Sabato, Universidad Nacional de San Martín, B1650KNA San Martín, Buenos Aires, Argentina*
[c]*Consejo Nacional de Investigaciones Científicas y Técnicas, Argentina*

Electrochemical impedance spectroscopy (EIS) tests were performed on alloy 22 in chloride and chloride plus inhibitor naturally aerated solutions, at 90°C. A R_Ω-(R_F//CPE) equivalent circuit model was used for fitting to the EIS data. R_Ω and R_F were the ohmic and film resistances, respectively, and CPE accounted for the non-ideal capacitance. The fitting errors of the circuit parameters decreased as pH increased. The passive film properties improved as pH increased from pH 0 to pH 4. At higher pH values, the passive film properties depended mainly on the identity of the salt added. Oxalic, picric and citric acids additions were detrimental for the passive film developed on alloy 22. Carbonate and bicarbonate led to less protective passive films only when added to 1 M NaCl solutions. Fluoride was a detrimental addition at pH 6, but not at pH 9. Acetic acid, carbonic acid, silicate, tungstate, and molybdate additions did not modify significantly the protective properties of the alloy 22 passive film. Nitrate, sulfate and chromate additions led to thick and protective passive films. The efficiency of the tested species as crevice corrosion inhibitors was not related to their effects on alloy 22 passivity.
 [DOI: 10.1149/2.040211jes]

Manuscript submitted July 2, 2012; revised manuscript received August 13, 2012. Published August 31, 2012.

Alloy 22 (UNS N06022) belongs to the Ni-Cr-Mo family. It shows an outstanding corrosion resistance in highly-corrosive conditions.[1] Alloy 22 develops a chromium-rich passive film which protects the alloy against corrosion by isolating it from the corrosive environment. The passivity and the localized corrosion resistance of alloy 22 have been studied in detail, due to its potential application as an engineered barrier of nuclear repositories.[2] Alloy 22 shows a very low corrosion rate in the passive state and it is highly resistant to stress corrosion cracking, pitting corrosion and crevice corrosion in hot chloride solutions.[1,2]

Electrochemical impedance spectroscopy (EIS) has been used to study alloy 22 passive film in a wide range of chloride concentrations, pH values and in the presence of other species.[3–18] In most of the cases, this alloy/environment system is well represented by a R_Ω-(R_F//CPE) circuit model, where R_Ω is the ohmic resistance, R_F is the film resistance and CPE accounts for a non-ideal capacitance.[6,10–17] The good fit of this equivalent circuit to EIS data means that the data are reliable, as this circuit fulfills a *priori* the Kramers-Kronig transformation.[19] Two time constants were observed at the beginning and at the end of the passive range.[6,14,17] They may also appear at short immersion times and in low pH solutions.[16,17] In these cases, the resistances for the ion transfer might be located at the film interfaces, and not in the film itself.[17] Surface analyzes studies indicate that the passive film barrier layer is made of Cr_2O_3 while Mo and W oxides are enriched in the outer regions of the film.[20,21] The protective properties of the film improve with polarization time due to the thickening and the aging of the film.[5,14,17] The film resistance and the space charge layer thickness increase with the applied potential up to a certain point, then they begin to decrease.[17,18] This decrease has been attributed to the further oxidation of the metal ions resulting in an increase of point defects in the film.[18] The passive film of alloy 22 is an n-type semiconductor, changing to a p-type at high passive potentials. The oxidation of Cr^{3+} to Cr^{6+} occurs within the film at high potentials, followed by transpassive dissolution.[3,5,7–9,14–18]

Alloy 22 is almost immune to pitting corrosion but it may be prone to crevice corrosion in aggressive environmental conditions, such as high chloride concentrations and high temperatures.[2,22] Certain species act as localized corrosion inhibitors which may mitigate or avoid the chloride-induced crevice corrosion on alloy 22.[22,23] Anodic inhibitors of the chloride-induced crevice corrosion of alloy 22 have been thoroughly studied.[24–33] Nitrate, sulfate, carbonate, phosphate, chromate, molybdate, tungstate, fluoride, hydroxyl, and organic acids may mitigate or inhibit this kind of localized attack. Crevice corrosion may occur only if the corrosion potential of the alloy (E_{CORR}) is higher than its repassivation potential ($E_{R,CREV}$) in the field conditions.[2,22] When these species are added in sufficient amounts to chloride solutions, they produce an increase of $E_{R,CREV}$. If the inhibitor to chloride ratio is higher than a critical value crevice corrosion is completely inhibited.[23] Chloride-induced crevice corrosion occurs due to the formation of a hydrochloric acid solution within the crevice. Anodic inhibitors avoid the development of hydrochloric acid or hamper its deleterious action.[23] Table I shows the inhibitor concentration needed for a complete inhibition of the chloride-induced crevice corrosion of alloy 22, at 90°C. Nitrate, phosphate and hydroxyl inhibit crevice corrosion at low concentrations, but large amounts of fluoride and organic acids are needed to have a similar effect.[24–27,29–31,33] Some inhibitors, such as fluoride and oxalic acid, may cause an increase of the passive current density if added in large amounts.[29,31,34] There is a lack of data regarding the effects of crevice corrosion inhibitors on the properties of alloy 22 passive film. The passive dissolution mechanism for crevice corrosion initiation assumes that localized acidification in the crevice occurs by cation hydrolysis, at a rate determined by the passive current density.[35] Consequently, those species which produce a decrease of the passive film resistance are not expected to be crevice corrosion inhibitors.

The objective of the present work was to assess the effect of crevice corrosion inhibitors on the passive film properties of alloy 22. A correlation was sought between the inhibitor efficiency and the passive film properties. Electrochemical impedance spectroscopy was used for obtaining information of the passive film formed on alloy 22 in chloride solutions and chloride plus inhibitor solutions, at 90°C. The inhibitors concentrations used were usually those associated with a complete crevice corrosion inhibition or even higher. The selection of the tested conditions was made based on the data gathered through ten years of research on crevice corrosion inhibitors.[6,23,29,31,32]

Experimental

Alloy 22 (N06022) prismatic specimens were prepared from wrought mill annealed plate stock. The chemical composition of the alloy in weight percent was 59.56% Ni, 20.38% Cr, 13.82% Mo, 2.64% W, 2.85% Fe, 0.17% V, 0.16% Mn, 0.008% P, 0.0002% S, 0.05% Si, and 0.005% C (Heat 059902LL1). The alloy was used in the mill annealed condition. Prismatic specimens are a variation of the ASTM G 5[36] specimen, which contains an artificial crevice formed by a PTFE compression gasket. The tested surface area was approximately 10 cm^2. The specimens had a finished grinding of abrasive paper number 600 and were degreased in acetone and washed in distilled water within the hour prior to testing.

[z]E-mail: maalrodr@cnea.gov.ar

Table I. Inhibitor concentration for a complete crevice corrosion inhibition of alloy 22 in chloride solutions at 90°C.[23] NS: not studied; NCI: no complete inhibition at the studied concentrations.

Inhibitor	0.1 M NaCl	1 M NaCl
Nitrate	0.02 M	0.2 M
Hydroxyl	0.032 M	0.032 M
Phosphate	NS	0.3 M
Chromate	0.05 M	1 M
Molybdate	0.05 M	NCI
Carbonate	0.1 M	1 M
Sulfate	0.1 M	2 M
Fluoride	0.5 M	NCI
Acetic Acid	1 M	NCI
Oxalic Acid	0.2 M	NCI
Citric Acid	0.2 M	NCI

Electrochemical tests were conducted in a one-liter three-electrode vessel (ASTM G 5).[36] A water-cooled condenser was used to avoid evaporation of the solution. The temperature of the solution was maintained at 90°C by immersing the cell in a water bath, which was kept at a constant temperature. All the tests were performed at ambient pressure. The reference electrode was a saturated calomel electrode (SCE), which has a potential of 0.242 V more positive than the standard hydrogen electrode (SHE). The reference electrode was connected to the solution through a water-cooled Luggin probe. The reference electrode was kept at room temperature. The electrode potentials were not corrected for the thermal liquid junction potential, since it was assumed to be on the order of a few mV.[37] The counter electrode consisted in a flag of platinum foil (total area 50 cm^2) spot-welded to a platinum wire. All the potentials in this paper are reported in the SCE scale.

Table II shows all the testing solutions along with their denominations in the present paper. The testing solutions contain NaCl plus a sodium salt or an organic acid. Pure NaCl solutions with different pH values were also used. The chloride concentrations of the solutions were 0.1 M or 1 M, with the exception of 0.5 M NaCl + 0.5 M NaF solutions. In those cases were the pH was adjusted, small volumes of HCl or NaOH were added to the solutions. The solutions containing Na_2CO_3, $NaHCO_3$, and H_2CO_3 were prepared from $NaHCO_3$ and their pH was also adjusted by the previously described procedure. The selected pH values were those corresponding to the maximum concentration of CO_3^{2-}, HCO_3^- and H_2CO_3, at 90°C (pH 11.5, 7 and 3, respectively).[38] The solutions containing Na_2SiO_3, $NaNO_3$, Na_2SO_4, Na_2CrO_4, Na_2MoO_4, Na_2WO_4, oxalic acid ($H_2C_2O_4$), acetic acid ($C_2H_4O_2$), citric acid ($C_6H_8O_7$) and picric acid ($C_6H_3N_3O_7$) were used at the pH values determined by their corresponding salts and/or acid hydrolysis.

The open circuit potential or corrosion potential of alloy 22 in the testing solutions was monitored for 24 hours under naturally aerated conditions. After this period of time, the EIS measurements were performed. A Solartron SI 1260 impedance/gain-phase analyzer coupled to a Solartron SI 1287 electrochemical interface potentiostat were used. A 10 mV amplitude sinusoidal potential signal was superimposed to the applied potential. The frequency scan was started at 10 kHz and ended at 1 mHz. Parameters of a simple equivalent circuit mathematical model were fitted to these data. The fits were performed with the software ZView 2 version 3.1c, from Scribner Associates, Inc. The errors reported for the fit parameters are those obtained with the software fitting tool. The equivalent circuit used in the present paper for fitting to the EIS experimental results is shown in Figure 1. This circuit included a Constant Phase Element (CPE) to deal with the frequency dispersion of the electrode.[19] Equation 1 was used for calculating the capacitance (C) of the electrode.[39] Q and α are the pre-exponential factor and the exponent of the CPE, respectively; R_Ω and R_F are the ohmic and the film resistances, respectively. Previous works have shown that Equation 1 give representative capacitance values for the studied system.[15–18] The topic of conversion from CPE to C has been recently discussed in the literature.[15,17,40] Other interpretations

Table II. Testing solutions used in the present work and their denominations.

pH	Solutions	Denomination
0.4	0.4 M HCl + 0.6 M NaCl	NaCl
1 to 9	1 M NaCl	
11 to 13	0.1 M NaCl	
10.8	0.1 M NaCl + 0.001 M Na_2SiO_3	NaCl + Na_2SiO_3
11.9	0.1 M NaCl + 0.01 M Na_2SiO_3	
12.5	0.1 M NaCl + 0.05 M Na_2SiO_3	
12.8	0.1 M NaCl + 0.1 M Na_2SiO_3	
3	0.1 M NaCl + 0.05 M H_2CO_3	NaCl + Na_2CO_3
3	0.1 M NaCl + 0.1 M H_2CO_3	
3	1 M NaCl + 0.2 M H_2CO_3	
3	1 M NaCl + 0.5 M H_2CO_3	
7	0.1 M NaCl + 0.1 M $NaHCO_3$	
7	0.1 M NaCl + 0.2 M $NaHCO_3$	
7	1 M NaCl + 1 M $NaHCO_3$	
7	1 M NaCl + 2 M $NaHCO_3$	
11.5	0.1 M NaCl + 0.1 M Na_2CO_3	
11.5	0.1 M NaCl + 0.2 M Na_2CO_3	
11.5	1 M NaCl + 1 M Na_2CO_3	
11.5	1 M NaCl + 2 M Na_2CO_3	
6	0.1 M NaCl + 0.02 M $NaNO_3$	NaCl + $NaNO_3$
6	0.1 M NaCl + 0.05 M $NaNO_3$	
6	1 M NaCl + 0.2 M $NaNO_3$	
6	1 M NaCl + 0.5 M $NaNO_3$	
6	0.1 M NaCl + 0.1 M Na_2SO_4	NaCl + Na_2SO_4
6	0.1 M NaCl + 0.2 M Na_2SO_4	
6	1 M NaCl + 1 M Na_2SO_4	
6	1 M NaCl + 2 M Na_2SO_4	
8	0.1 M NaCl + 0.05 M Na_2CrO_4	NaCl + Na_2CrO_4
8	0.1 M NaCl + 0.1 M Na_2CrO_4	
8	1 M NaCl + 0.5 M Na_2CrO_4	
8	1 M NaCl + 1 M Na_2CrO_4	
6.5	0.1 M NaCl + 0.05 M Na_2MoO_4	NaCl + Na_2MoO_4
7	0.1 M NaCl + 0.1 M Na_2MoO_4	
7.8	1 M NaCl + 0.5 M Na_2MoO_4	
8	1 M NaCl + 1 M Na_2MoO_4	
8	0.1 M NaCl + 0.1 M Na_2WO_4	NaCl + Na_2WO_4
8.5	0.1 M NaCl + 0.2 M Na_2WO_4	
10	1 M NaCl + 1 M Na_2WO_4	
11	1 M NaCl + 2 M Na_2WO_4	
6	0.5 M NaCl + 0.5 M NaF	0.5 M NaCl + 0.5 M NaF
9	0.5 M NaCl + 0.5 M NaF	
3	1 M NaCl + 0.001 M oxalic acid	NaCl + Oxalic Acid
2	1 M NaCl + 0.01 M oxalic acid	
3.7	1 M NaCl + 0.001 M acetic acid	NaCl + Acetic acid
3.3	1 M NaCl + 0.01 M acetic acid	
2.8	1 M NaCl + 0.1 M acetic acid	
3	1 M NaCl + 0.001 M citric acid	NaCl + Citric Acid
2.5	1 M NaCl + 0.01 M citric acid	
1.9	1 M NaCl + 0.1 M citric acid	
3	1 M NaCl + 0.001 M picric acid	NaCl + Picric Acid
2.1	1 M NaCl + 0.01 M picric acid	
1.5	1 M NaCl + 0.05 M picric acid	

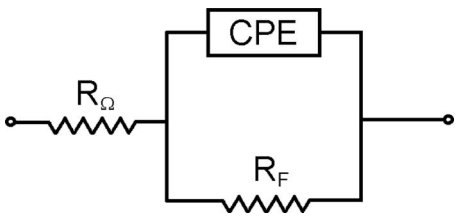

Figure 1. R_Ω-(R_F//CPE) equivalent circuit used for fitting to the EIS spectra. R_Ω is the ohmic resistance, R_F is the film resistance and CPE accounts for a non-ideal capacitance.

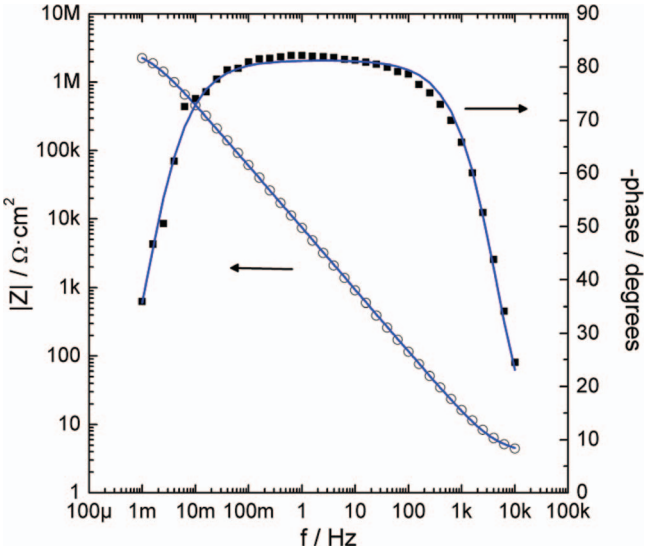

Figure 2. Bode diagram corresponding to an EIS test on alloy 22 after 24 hours of immersion in naturally aerated pH 6.3, 1 M NaCl + 1 M Na_2SO_4 at $E_{CORR} = -0.265$ V_{SCE}. Dots: experimental data; lines: fit.

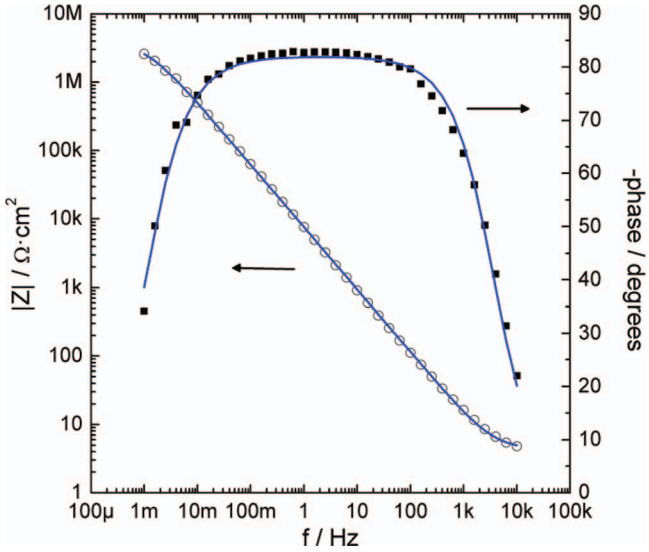

Figure 3. Bode diagram corresponding to an EIS test on alloy 22 after 24 hours of immersion in naturally aerated pH 8, 1 M NaCl + 1 M Na_2MoO_4 at $E_{CORR} = -0.307$ V_{SCE}. Dots: experimental data; lines: fit.

may be found.[40]

$$C = Q^{1/\alpha}\left(\frac{1}{R_\Omega} + \frac{1}{R_F}\right)^{\frac{(\alpha-1)}{\alpha}} \quad [1]$$

The value of C obtained from Equation 1 is the series combination of the space charge capacitance (C_{SC}) of the passive film and the double layer capacitance (C_{DL}).[17] C_{SC} was calculated according to Equation 2, assuming $C_{DL} = 30$ µF/cm².[17]

$$C_{SC} = \left(\frac{1}{C} - \frac{1}{C_{DL}}\right)^{-1} \quad [2]$$

The space charge layer thickness (d_{SC}) was obtained from C_{SC} by considering a parallel plate capacitor.[19] Equation 3 was used for this purpose, where ε_0 is the vacuum permittivity (8.85×10^{-14} F/cm) and ε is the dielectric constant of the film. $\varepsilon = 30$ was selected based on the literature.[4,10,12,15–18] The calculation of d_{SC} from Equation 3 may be subjected to error as ε may change with solution composition and potential.[41] However, these are good reference values since almost all the calculations in the literature were made by using $\varepsilon = 30$.

$$d_{SC} = \frac{\varepsilon_0 \varepsilon}{C_{SC}} \quad [3]$$

Results

Figures 2, 3, and 4 show Bode diagrams corresponding to EIS tests on alloy 22 after 24 hours of immersion in naturally aerated solutions containing NaCl plus different inhibitors. Measurements were performed at the corresponding corrosion potentials. Dots represent the experimental data, and lines represent the equivalent circuit fits. The measurements in pH 6.3, 1 M NaCl + 1 M Na_2SO_4, in pH 8, 1 M NaCl + 1 M Na_2MoO_4, and in pH 11.5, 0.1 M NaCl + 0.1 M Na_2CO_3 showed one time constant. They are representative of all the measurements performed in the present work. The equivalent circuit depicted in Figure 1 was used for fitting to the EIS data. This circuit showed a good fit to the data in a wide range of environmental conditions as reported elsewhere.[17] It was observed that the goodness of fit not only depended on the species in solution but also depended on the solution pH. Figures 5 and 6 show Chi^2 and the errors corresponding to equivalent circuit fits of α, Q and R_Ω as a function of pH. Chi^2 and the errors of α, Q and R_Ω showed a decrease as pH increased. Equation 4 was used for fitting Chi^2 and the errors of α, Q and R_Ω

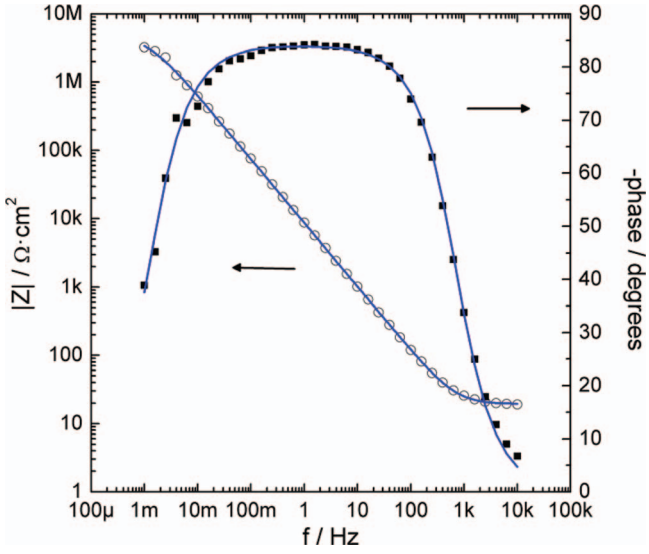

Figure 4. Bode diagram corresponding to an EIS test on alloy 22 after 24 hours of immersion in naturally aerated pH 11.5, 0.1 M NaCl + 0.1 M Na_2CO_3 at $E_{CORR} = -0.268$ V_{SCE}. Dots: experimental data; lines: fit.

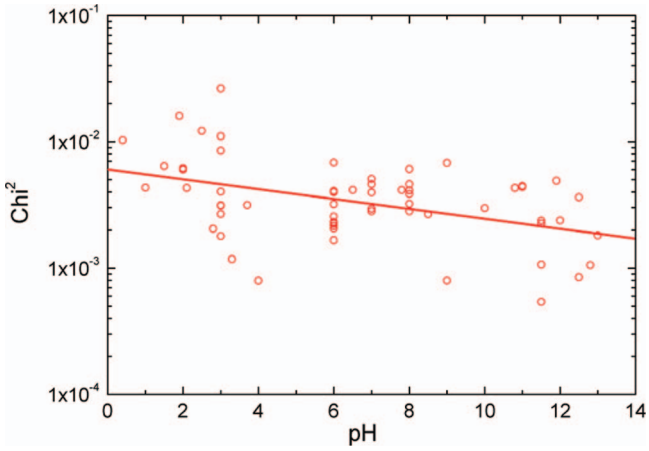

Figure 5. Chi^2 corresponding to equivalent circuit fits as a function of pH.

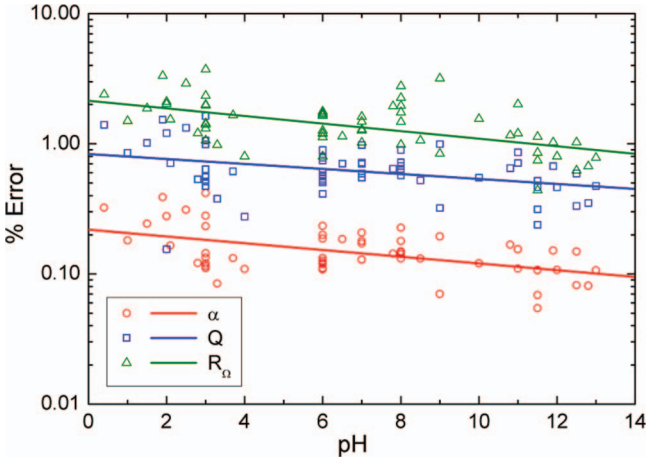

Figure 6. Errors corresponding to equivalent circuit fits of α, Q and R_Ω as a function of pH.

as a function of pH; where A and B are constants, and X represents any of the fitted variables (Chi^2, the errors of α, Q and R_Ω). Table III shows the fit parameters obtained for Equation 4. The negative slope ($A < 0$) for Chi^2 and the errors indicates that the equivalent circuit model had a better performance as pH increased.

$$\log(X) = ApH + B \quad [4]$$

Figure 7 shows R_F along with the corresponding error bars as a function of solution pH. The error of R_F becomes significant only for some measurements where $R_F > 3$ MΩ.cm^2 holds. The error of R_F was not a function of pH but it increased with R_F due to the error of measurement associated with low currents and the model extrapolation at low frequencies. R_F increased from pH 0 to pH 4 (Fig. 7). Chloride solutions containing organic acids showed lower R_F than pure chloride solutions of similar pH. Oxalic acid was the most detrimental among tested acids regarding passive film resistance. Carbonic acid additions did not produce a decrease of R_F when compared to pure chloride solutions. In the pH range from 4 to 13, R_F was a function of the species in solution, but not a function of pH (Fig. 7). The passive film resistance was higher or similar to that in pure chloride solutions when Na_2SiO_3, $NaNO_3$, Na_2SO_4, Na_2CrO_4, Na_2MoO_4 or Na_2WO_4 were added. NaF addition was deleterious for the passive film resistance, at pH 6. Na_2CO_3 (pH 11.5) and $NaHCO_3$ (pH 7) additions produced a decrease of R_F when tested in 1 M NaCl, but not in 0.1 M NaCl solutions.

Figure 8 shows the capacitance obtained from Equation 1, as a function of pH. C decreased from pH 0 to pH 4, showing an opposite trend with pH to that of R_F (Figs. 7 and 8). Chloride solutions containing organic acids showed higher C values than pure chloride solutions of similar pH. In the pH range from 4 to 13, C was a function of the species in solution, but not a function of pH (Fig. 8). This behavior mimics that of R_F but showing large C values for those tests where R_F values were small and vice versa. EIS tests in pure chloride solutions indicate that C and R_F are functions of potential.[17,18] C decreases as potential increases up to a certain point, and then it starts to decrease. R_F shows an opposite trend with potential to that of C, as observed in the present work (Figs. 7 and 8). The capacitances were lower

Table III. Fit parameters for Chi^2 and the errors of α, Q and R_Ω as a function of pH, according to Equation 4.

X	A	B	R^2
Chi^2	−0.039	−2.22	0.190
α	−0.026	−2.66	0.272
Q	−0.019	−2.08	0.125
R_Ω	−0.029	−1.67	0.288

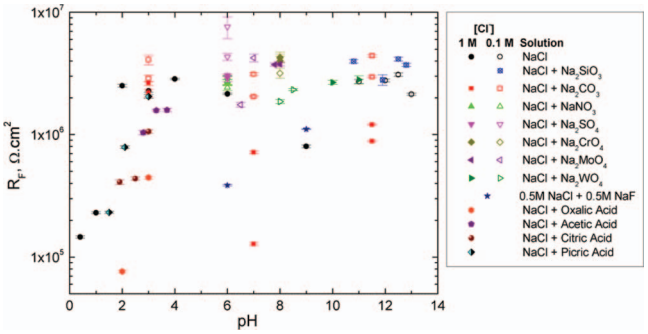

Figure 7. Passive film resistance from equivalent circuit fits as a function of pH.

or similar to that in pure chloride solutions when Na_2SiO_3, $NaNO_3$, Na_2SO_4, Na_2CrO_4, Na_2MoO_4 or Na_2WO_4 were added. Large capacitances were observed in those tests in pH 6, 0.5 M NaCl + 0.5 M NaF, and in pH 7 and pH 11.5, NaCl + Na_2CO_3 solutions. The passive film space charge layer capacitance was calculated from the obtained capacitance according to Equation 2. Figure 8 shows that there are three tests with $C > C_{DL}$. It was assumed that alloy 22 passive film in pH 2, 1 M NaCl + 0.01 M oxalic acid, in pH 1.9, 1 M NaCl + 0.1 M citric acid, and in pH 1.5, 1 M NaCl + 0.05 M picric acid was poorly developed. The film might not be covering the entire alloy surface but forming islands.[42] In these three tests referenced above, the equivalent circuit of Figure 1 is not physically correct since the double layer capacitance should be in parallel with the space charge capacitance. The description of these systems is out of the scope of the present work.

Figure 9 shows the space charge layer thickness calculated from Equation 3, as a function of solution pH. The space layer thickness and the entire passive film thickness might not be exactly the same. However, they were assumed to follow the same trend with environmental variables changes (changes in pH and solution composition). The thickness of a Cr_2O_3 monolayer formed on Ni-Cr alloys is 0.21 nm.[43] This is indicated in Figure 9 with a dash line. The present calculations should be considered semiquantitative because of the error involved in the assumption of a constant value for ε (Eq. 3). EIS measurements in 0.4 M HCl + 0.6 M NaCl, in pH 2.5, 1 M NaCl + 0.01 M citric acid, and in pH 2.1, 1 M NaCl + 0.01 M picric acid showed $d_{SC} < 0.21$ nm. The Cr_2O_3 barrier layer might be not fully developed in these conditions. Ni, Mo and/or W might be the main constituents of these passive films. Surface analyzes techniques should be used to determine the passive film composition in these conditions. d_{SC} increased from pH 0 to pH 4 (Fig. 9). In the pH range from 4 to 13, d_{SC} was a function of the species in solution, but not a function of pH (Fig. 9). The presence of oxalic, citric and picric acids led to thinner films than those in pure chloride solutions of similar pH. Acetic acid additions did not produce a decrease of d_{SC}. Carbonic acid

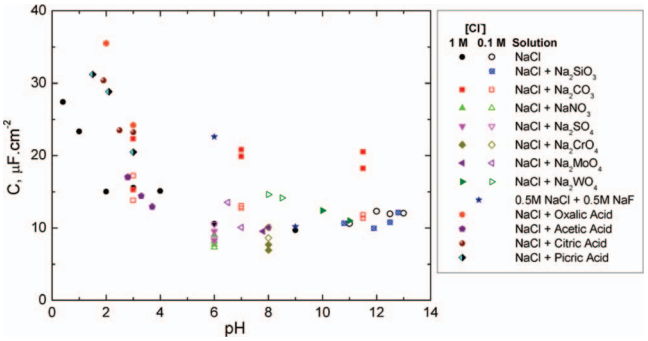

Figure 8. Capacitance from EIS tests as a function of pH.

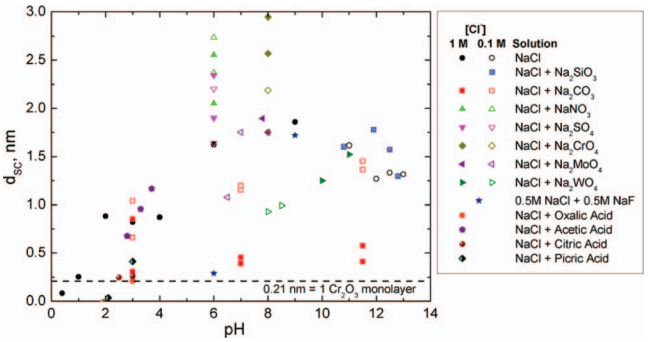

Figure 9. Passive film space charge thickness as a function of pH.

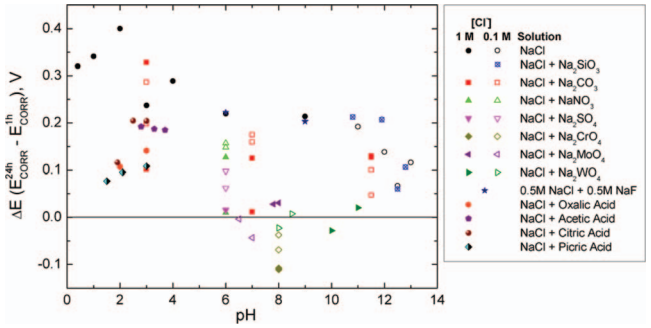

Figure 11. Corrosion potential ennoblement from 1 to 24 hours of immersion in naturally aerated solutions at 90°C as a function of pH.

additions did not produce a decrease of d_{SC} with the only exception of the pH 3, 1 M NaCl + 0.5 M H_2CO_3 solution (Fig. 9). In the pH range from 4 to 13, d_{SC} varied from 0.3 nm to 3 nm depending on the species in solution. The thinnest films were those formed in the pH 6, 0.5 M NaCl + 0.5 M NaF solution, and in the 1 M NaCl solutions containing $NaHCO_3$ (pH 7) and Na_2CO_3 (pH 11.5). The thicker films were those formed in chloride solutions with Na_2CrO_4, $NaNO_3$, and Na_2SO_4 additions. The chemical identity of the species greatly influenced the film thickness. For instance, d_{SC} varied from 0.3 nm to 2.7 nm at pH 6, depending on the salt added to the chloride solution (Fig. 9).

Figure 10 shows the corrosion potential of alloy 22 at 24 hours of immersion, as a function of pH. Relevant data from literature in pure chloride solutions at 90°C are also plotted to put into context the obtained values.[17,44] The linear fit of E_{CORR} vs. pH is shown in Equation 5 and in Figure 10. All the E_{CORR} values at 24 hours of immersion from the present work were considered in the fit.

$$E_{CORR}(V_{SCE}) = -0.040\ pH + 0.088 \quad (R^2 = 0.645) \qquad [5]$$

E_{CORR} showed an average decrease of 40 mV/pH unit. E_{CORR} was also a function of the chemical species added to the chloride solution. In general, the pure chloride solutions showed higher E_{CORR} than the chloride solutions with acid or salt additions. E_{CORR} was well above the passive film flatband potential (E_{FB}) determined in pure chloride solutions (Figure 10).[17] E_{FB} may change with the addition of inhibitors to the solution but it is mainly pH dependent. Alloy 22 passive film is expected to behave as an n-type semiconductor in the tested conditions, at pH < 9. At higher pH values, p-type semiconduction is inferred. This is an extrapolation as there is no available information above pH 6.[17] The development of the passive film and its type of semiconduction may affect the kinetics of the cathodic reactions on the film.[45] The crevice corrosion repassivation potential of alloy 22 in pure chloride solutions, at 90°C, is between −0.200 V_{SCE} (10 M Cl^-) and −0.120 V_{SCE} (0.1 M Cl^-).[44] This

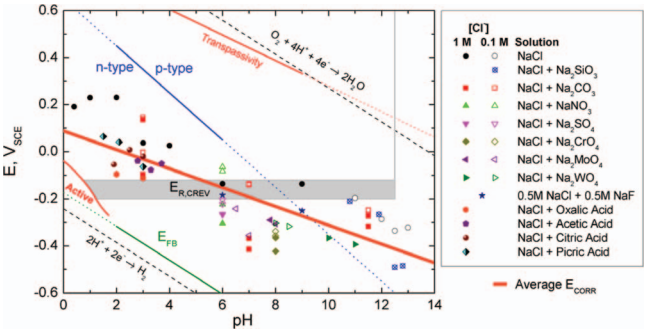

Figure 10. Corrosion potential at 24 hours of immersion in naturally aerated solutions at 90°C as a function of pH. Relevant data of Alloy 22 in pure chloride solutions from literature is also shown.[17,44]

range of $E_{R,CREV}$ is also shown in Figure 10. No crevice corrosion has been reported above pH 12.5.[32] The environmental range of crevice corrosion susceptibility in the absence of inhibitors is above $E_{R,CREV}$ and below pH 12.5 (Fig. 10). Considering an average value of $E_{R,CREV}$ = −0.160 V_{SCE}, it comes that below pH 6.2, $E_{CORR} > E_{R,CREV}$ holds and crevice corrosion would be possible in the absence of inhibitors. Care must be taken in extrapolating this result since crevice corrosion will only occur if a tight crevice is formed on the alloy surface and the cathodic reactions occur at a rate high enough to supply electrons to the anodic process.[23,46]

Figure 11 shows the E_{CORR} ennoblement (ΔE) as a function of pH. ΔE was defined as the difference between E_{CORR} at 24 hours of immersion (E_{CORR}^{24h}) and E_{CORR} at 1 hour of immersion (E_{CORR}^{1h}). ΔE is usually associated with the improvement of the passive film properties.[6,14,16] In the range from pH 0 to pH 4, large positive ΔE were observed. Pure chloride solutions led to ΔE from 0.24 V to 0.40 V. Chloride solutions with organic acid additions led to ΔE from 0.08 V to 0.21 V. Chloride solutions with H_2CO_3 additions led to ΔE from 0.10 V to 0.33 V. In the pH range from 4 to 13, ΔE values from −0.10 V to 0.20 V were observed, depending on the salt added to the chloride solution. In general, pure chloride solutions led to higher ΔE than chloride solutions with salt additions. NaCl + Na_2CrO_4 solutions led to the lowest ΔE (ΔE < 0). NaCl + Na_2MoO_4 and NaCl + Na_2WO_4 solutions also led to negative or very small ΔE. 0.5 M NaCl + 0.5 M NaF solutions and NaCl + Na_2SiO_3 solutions led to ΔE values similar to those of pure chloride solutions. Chloride solutions containing Na_2CO_3, $NaNO_3$ and Na_2SO_4 led to ΔE from 0.01 V to 0.20 V, depending on the salt concentration.

Discussion

The behavior of passive alloy 22 in chloride solutions and chloride plus crevice corrosion inhibitor solutions may be analyzed in two different pH ranges:

- In the range from pH 0 to pH 4, the film resistance and the space charge layer thickness increased as pH increased, E_{CORR} at 24 hours largely exceeded $E_{R,CREV}$, significant E_{CORR} ennoblement were observed and the passive film was an n-type semiconductor.
- In the range from pH 4 to pH 13, the film resistance, the space charge layer thickness and E_{CORR} ennoblement did not depend on pH but on the identity of the salt added to the chloride solutions, E_{CORR} at 24 hours were in the range of $E_{R,CREV}$ or below and the passive film is expected to change from n-type to p-type semiconductor.

In the range from pH 0 to pH 4, the passive film of alloy 22 showed different properties in pure chloride solutions than in chloride solutions with some organic acid additions. Oxalic acid produced a significant decrease in the passive film resistance and thickness (Figs. 7 and 9). At pH 2, the passive film was poorly developed in the chloride plus oxalic acid solution while the film in the pure chloride solution showed high resistance and E_{CORR}, and a significant E_{CORR}

ennoblement (Figs. 7-10). Oxalic acid was the most detrimental for alloy 22 passivity among tested acids. Additions of picric and citric acids also led to lower film resistances and thicknesses (Figs. 7 and 9). Picric acid reduction reaction is expected to occur in the tested conditions.[31] Acetic and carbonic acid additions did not affect significantly the passive film properties compared with pure chloride solutions (Figs. 7-10). Organic acids are weak crevice corrosion inhibitors since large inhibitor to chloride concentration ratios are needed for a complete inhibition (Table I). The inhibitor efficiencies are neither associated to the dissociation constants of the acids, nor to their buffer capacities or to their molecular sizes.[31] Although $E_{R,CREV}$ is not a strong function of solution pH, alloy 22 has been found more prone to crevice corrosion at low pH, in open circuit conditions.[47] This may be due to the thinner passive film enabling cathodic reactions at a high rate to support the crevice corrosion. EIS tests on alloy 22 in chloride plus organic acid solutions in higher concentrations than those used in the present work show a second time constant.[31] In the present work, Chi^2 and the errors of most of the fit parameters were higher in the low pH range (Figs. 5 and 6). The presence of a second time constant in EIS tests at low pH may be the cause of the higher errors of these fits. In three of the tests at low pH (those with $C > C_{DL}$, Fig. 8), the proposed model failed to describe the physical situation as the passive film was not developed over the entire alloy surface.

In the range from pH 4 to pH 13, the passive film properties depended mainly on the identity of the salt added to the chloride solution. SiO_3^{2-} addition did not influence significantly the passive behavior of alloy 22 when compared to pure chloride solutions (Figs. 7–11). HCO_3^- (pH 7) and CO_3^{2-} (pH 11.5) produced a decrease of the film resistance and thickness when added to 1 M NaCl solutions. These anions in conjunction with chloride have been identified as promoters of stress corrosion cracking of alloy 22.[38] Stress corrosion cracking may occur at potentials around 0.2 V_{SCE} at pH 7, and around 0.1 V_{SCE} at pH 11.5. These potentials are higher than the E_{CORR} of alloy 22 in the present work (Fig. 10). However, the present results clearly indicate that the passive film was thinner and less protective in concentrated chloride plus HCO_3^-/CO_3^{2-} solutions. Fluoride was a detrimental addition for alloy 22 passive film at pH 6, but not at pH 9. Alloy 22 showed a thinner and less protective film in pH 6, 0.5 M NaCl + 0.5 M NaF than in a pure chloride solution of the same pH (Figs. 7 and 9). NO_3^- and SO_4^{2-} additions to chloride solutions led to thicker and more protective passive films than those formed in pure chloride solutions (Figs. 7 and 9). These higher film thicknesses were not associated with higher E_{CORR} values or E_{CORR} ennoblements when compared to pure chloride solutions (Figs. 10 and 11). Although, NO_3^- is expected to be oxidizing and SO_4^{2-} is not,[48] there were no differences among their E_{CORR} (Fig. 10). NO_3^- and SO_4^{2-} might decrease the rate of chemical dissolution of the passive film.

CrO_4^{2-}, MoO_4^{2-}, and WO_4^{2-} produced protective passive films when added to chloride solutions (Fig. 7). Their addition led to lower E_{CORR} values and E_{CORR} ennoblements. CrO_4^{2-} and MoO_4^{2-} may be oxidizing. CrO_4^{2-} and MoO_4^{2-} may reduce according to Equations 6 and 7, respectively.[48] However, the reaction products in the tested conditions might be hydrated species, such as $Cr(OH)_3$ and CrOOH for Equation 6, and $Mo(OH)_4$, $MoO(OH)_2$ for Equation 7.[48]

$$CrO_4^{2-} + 5H^+ + 3e^- \rightarrow {}^1/_2Cr_2O_3 + {}^5/_2H_2O \quad [6]$$

$$MoO_4^{2-} + 4H^+ + 2e^- \rightarrow MoO_2 + 2H_2O \quad [7]$$

Reduction of CrO_4^{2-} leads to the formation of $Cr(OH)_3$/CrOOH/Cr_2O_3 which may be built into the film (Eq. 6). Equation 6 is thermodynamically possible in the tested conditions.[48] The thickness of alloy 22 passive film increased with the concentration of CrO_4^{2-} (Fig. 9). This suggests that the Cr^{3+} species formed *via* Equation 6 was effectively built into the film. The increase of the film thickness may have produced the inhibition of cathodic reactions avoiding the E_{CORR} ennoblement (Fig. 11) and leading to low E_{CORR} values (Fig. 10). Reduction of MoO_4^{2-} *via* Equation 7 results in the formation of solid $Mo(OH)_4/MoO(OH)_2/MoO_2$. Comparison of E_{CORR} with thermodynamic data at room temperature led to the conclusion that Equation 7 may only proceed in pH 7.8, 1 M NaCl + 0.5 M Na_2MoO_4 and in pH 8, 1 M NaCl + 1 M Na_2MoO_4 solutions.[48] However, the negative values of ΔE observed implies that E_{CORR} was higher at shorter immersion times (Fig. 11). Consequently, MoO_4^{2-} might be also oxidizing in dilute solutions. MoO_4^{2-} addition did not increase the film thickness (Fig. 9). It suggests that the Mo^{4+} species formed *via* Equation 7 was not incorporated into the film barrier layer. On the other hand, WO_4^{2-} is not oxidizing in the tested conditions.[48] WO_4^{2-} addition to chloride solutions led to slightly thinner passive films, moderate E_{CORR} and low or negative ΔE (Figs. 9–11).

According to the passive dissolution mechanism for crevice corrosion initiation, the rate of the localized acidification is directly proportional to passive current density.[35] Consequently, crevice corrosion inhibitors should increase the passive film resistance while detrimental species should decrease it. In the present work, it was found that oxalic and citric acids were detrimental for the alloy passivity, while acetic acid did not produce a decrease of the film resistance. However, oxalic and citric acids are reported to be more efficient crevice corrosion inhibitors than acetic acid (Table I). Carbonic acid is not a crevice corrosion inhibitor of alloy 22.[23] This acid was not detrimental for alloy 22 passive film in the conditions tested in the present work. It is reported that nitrate and chromate are efficient crevice corrosion inhibitors (Table I). In the present work, they led to very resistant passive films when added to chloride solutions (Figs. 7 and 9). Literature data indicate that sulfate and carbonate are crevice corrosion inhibitors of similar efficiency (Table I). However, sulfate promoted a thick and very resistant passive film, while carbonate led to a thin and less protective film when added to concentrated chloride solutions (Figs. 7 and 9). Molybdate is reported to be an efficient inhibitor in 0.1 M NaCl solutions, but it shows a poor performance in 1 M NaCl solutions (Table I). However, the present results showed that the effect of molybdate on alloy 22 passivity did not depend on the chloride concentration. It has been stated that fluoride is a weak crevice corrosion inhibitor in pH 6 chloride solutions (Table I).[29,34] Present results showed that fluoride was detrimental to the alloy passivity in the same conditions (Figs. 7 and 9). Silicate and tungstate have not shown significant properties as crevice corrosion inhibitors.[23,32] However, in the present work, they led to protective passive films when added to chloride solutions (Figs. 7 and 9).

The comparison of the present results on the influence of the tested species on alloy 22 passivity and their efficiencies as crevice corrosion inhibitors do not lead to any obvious relationship. Crevice corrosion inhibitors such as oxalic acid, citric acid, fluoride and carbonate may adversely affect the passive film resistance. Other species, such as carbonic acid, silicate and tungstate produced a resistant film but they are not crevice corrosion inhibitors. There are also crevice corrosion inhibitors, such as nitrate, chromate, molybdate and sulfate, which promote protective passive films.

Conclusions

Electrochemical impedance spectroscopy measurements were performed on alloy 22 after 24 hour of immersion, in naturally aerated chloride solutions and chloride plus inhibitor solutions, at 90°C. A R_Ω-(R_F//CPE) circuit model was used for fitting. The goodness of fit increased with solution pH.

In the range from pH 0 to pH 4, the passive film properties improved as pH increased. In the range from pH 4 to pH 13, the passive film properties did not depend on pH but on the identity of the salt added to the chloride solutions.

Additions of oxalic, picric and citric acids to chloride solutions led to lower film resistances and thicknesses. Additions of acetic and carbonic acids did not affect significantly the passive film properties compared with pure chloride solutions. Carbonate and bicarbonate produced a decrease of the film resistance and thickness when added to 1 M NaCl solutions. These anions did not show any detrimental effect on passivity when added to 0.1 M NaCl solutions. Fluoride

was a detrimental addition for alloy 22 passive film at pH 6, but not at pH 9. Nitrate and sulfate additions to chloride solutions led to thicker and more protective passive films than those formed in pure chloride solutions. Chromate additions led to protective passive films and their thickness increased with the chromate concentration. Silicate, tungstate, and molybdate did not modify significantly the protective properties of alloy 22 passive film.

There was not an obvious relationship between the influence of the tested species on alloy 22 passivity and their efficiencies as crevice corrosion inhibitors.

Acknowledgments

Financial support from the Agencia Nacional de Promoción Científica y Tecnológica of the Ministerio de Ciencia, Tecnología e Innovación Productiva from Argentina and from the Universidad Nacional de San Martín is acknowledged.

References

1. R. B. Rebak, *Corrosion and Environmental Degradation*, Volume **II**, Wiley-VCH, Weinheim, Germany (2000).
2. G. M. Gordon, *Corrosion*, **58**, 811 (2002).
3. G. Bellanger and J. J. Rameau, *Journal of Material Science*, **31**, 2097 (1996).
4. D. D. Macdonald, A. Sun, N. Priyantha, and P. Jayaweera, *J. Electroanal. Chem.*, **572**, 421 (2004).
5. N. Priyantha, P. Jayaweera, D. D. Macdonald, and A. Sun, *J. Electroanal. Chem.*, **572**, 409 (2004).
6. M. A. Rodríguez, R. M. Carranza, and R. B. Rebak, *Metallurgical and Materials Transactions A*, **36A**(5), 1179 (2005).
7. K. S. Raja, S. A. Namjoshi, and M. Misra, *Materials Letters*, **59**, 570 (2005).
8. D. D. Macdonald and A. Sun, *Electrochim. Acta*, **51**, 1767 (2006).
9. K. S. Raja and D. A. Jones, *Corros. Sci.*, **48**, 1623 (2006).
10. J. J. Gray, J. R. Hayes, G. E. Gdowski, B. E. Viani, and C. A. Orme, *J. Electrochem. Soc.*, **153**(3), B61 (2006).
11. J. J. Gray, J. R. Hayes, G. E. Gdowski, and C. A. Orme, *J. Electrochem. Soc.*, **153**(5), B156 (2006).
12. J. J. Gray, B. S. El Dasher, and C. A. Orme, *Surf. Sci.*, **600**, 2488 (2006).
13. J. J. Gray and C. A. Orme, *Electrochim. Acta*, **52**, 2370 (2007).
14. M. A. Rodríguez, R. B. Rebak, and R. M. Carranza, in *Materials Research Society Symposium Proceedings* Vol. **985**, MRS, Warrendale, PA, p. 287 (2007).
15. S. P. Harrington and T. M. Devine, *J. Electrochem. Soc.*, **156**(4), C154 (2009).
16. M. A. Rodríguez, R. M. Carranza, and R. B. Rebak, *J. Electrochem. Soc.*, **157**(1), C1 (2010).
17. M. A. Rodríguez and R. M. Carranza, *J. Electrochem. Soc.*, **158**(6), C221 (2011).
18. P. Jakupi, D. Zagidulin, J. J. Noël, and D. W. Shoesmith, *Electrochim. Acta*, **56**, 6251 (2011).
19. E. Barsoukov and J. R. Macdonald, *Impedance Spectroscopy: Theory, Experiment, and Applications*, 2nd ed., John Wiley & Sons, Hoboken, NJ (2005).
20. A. C. Lloyd, D. W. Shoesmith, N. S. MacIntyre, and J. J. Noël, *J. Electrochem. Soc.*, **150**(4), B120 (2003).
21. A. C. Lloyd, J. J. Noël, N. S. MacIntyre, and D. W. Shoesmith, *Electrochim. Acta*, **49**, 3015 (2004).
22. R. M. Carranza, *Journal of Metals*, **60**, 58 (2008).
23. M. A. Rodríguez, *Corros. Rev.*, **30**, 19 (2012).
24. B. A. Kehler, G. O. Ilevbare, and J. C. Scully, *Corrosion*, **57**, 1042 (2001).
25. G. O. Ilevbare, K. J. King, S. R. Gordon, H. A. Elayat, G. E. Gdowski, and T. S. E. Gdowski, *J. Electrochem. Soc.*, **152**, B547 (2005).
26. D. S. Dunn, Y.-M. Pan, K. Chiang, L. Yang, G. A. Cragnolino, and X. He, *Journal of Metals*, **57**, 49 (2005).
27. D. S. Dunn, Y.-M. Pan, L. Yang, and G. A. Cragnolino, *Corrosion*, **62**, 3 (2006).
28. G. O. Ilevbare, *Corrosion*, **62**, 340 (2006).
29. R. M. Carranza, M. A. Rodríguez, and R. B. Rebak, *Corrosion*, **63**, 480 (2007).
30. A. K. Mishra and G. S. Frankel, *Corrosion*, **64**, 836 (2008).
31. R. M. Carranza, C. M. Giordano, M. A. Rodríguez, and R. B. Rebak, Paper N° 08578, Corrosion/2008, NACE Intl., Houston, TX (2008).
32. R. M. Carranza, M. Rincón Ortíz, M. A. Rodríguez, and R. B. Rebak, "Corrosion resistance of Alloy 22 in chloride and silicate solutions", *14th International Conference on Environmental Degradation of Materials in Nuclear Power Systems-Water Reactors*, August 23-27, ANS, Virginia Beach, VA (2009).
33. M. Miyagusuku, R. M. Carranza, and R. B. Rebak, Paper N° 10238, Corrosion/2010, NACE Intl., Houston, TX (2010).
34. R. M. Carranza, M. A. Rodríguez, and R. B. Rebak, in *Materials Research Society Symposium Proceedings* Vol. **1124**, MRS, Warrendale, PA, p. 487 (2009).
35. J. W. Oldfield and W. H. Sutton, *Br. Corros. J.*, **13**, 13 (1978).
36. ASTM International, *Annual Book of ASTM Standards: Wear and Erosion; Metal Corrosion*, Vol. **03.02**, ASTM International, West Conshohocken, PA (2005)
37. D. D. Macdonald, A. C. Scott, and P. Wentrcek, *J. Electrochem. Soc.*, **126**(6), 908 (1979).
38. P. K. Shukla, D. S. Dunn, K.-T. Chiang, and O. Pensado, Paper N° 06502, Corrosion/2006, NACE Intl., Houston, TX (2006).
39. G. J. Brug, A. L. G. Van Den Eeden, M. Sluyters-Rehbach, and J. H. Sluyters, *J. Electroanal. Chem.*, **176**, 275 (1984).
40. B. Hirschorn, M. E. Orazem, B. Tribollet, V. Vivier, I. Frateur, and M. Musiani, *Electrochim. Acta*, **55**, 6218 (2010).
41. T. P. Moffat and R. M. Latanision, *J. Electrochem. Soc.*, **139**, 1869 (1992).
42. P. Marcus and V. Maurice, *Corrosion and Environmental Degradation*, Volume **II**, Wiley-VCH, Weinheim, Germany (2000).
43. S. Boudin, J.-L. Vignes, G. Lorang, M. Da Cunha Belo, G. Blondiaux, S. M. Mikhailov, J. P. Jacobs, and H. H. Brongersma, *Surf. Interface Anal.*, **22**, 462 (1994).
44. M. Rincón Ortíz, M. A. Rodríguez, R. M. Carranza, and R. B. Rebak, *Corrosion*, **66**, 105002 (2010).
45. K. V. Rybalka, L. A. Beketaeva, and A. D. Davydov, *Corros. Sci.*, **54**, 161 (2012).
46. P. Jakupi, J. J. Noël, and D. W. Shoesmith, *Corros. Sci.*, **53**, 3122 (2011).
47. M. A. Rodríguez, R. M. Carranza, and R. B. Rebak, Paper N° 09424, Corrosion/2009, NACE Intl., Houston, TX (2009).
48. M. Pourbaix, *Atlas of electrochemical equilibria in aqueous solutions*, NACE Intl., Houston, TX (1974).